WOOD RESEARCH
63 (6): 2018
979-992

SEISMIC EVALUATION OF WOOD FRAME CONSTRUCTION BASED ON NAIL CONNECTION DEFLECTION STATUS

Yingyang Liu
Zhengzhou University, School of Civil Engineering
Zhengzhou, China

Haibei Xiong
Tongji University
Shanghai, China

Jiahua Kang
Architectural Design & Research Institute
of Tongji University (Group) Co., Ltd.
Shanghai, China

(Received November 2017)

ABSTRACT

This paper presents a concept for a seismic evaluation method for wood frame construction based on analyzing the nail connection performance status. An empirical nail model adjusted using an energy equivalence principle is proposed and experimentally validated. Then, a pushover analysis is conducted on a finite element model of a wood frame construction with a practical configuration, and the structural performances under different seismic hazard levels are evaluated based on the indicators given by FEMA 273. With the methodology proposed in this paper, engineers are able to directly perform an effective seismic evaluation by analyzing the nail connection performance status, from which the main nonlinearity of the wood frame construction originates.

KEYWORDS: Wood frame construction, seismic evaluation, performance-based design, nail connection, finite element method, pushover analysis.

INTRODUCTION

Because of the high strength-to-weight ratio of wood, the redundancy of structural systems, and the ductility of nail connections, wood frame construction is generally recognized as being

able to perform well in seismic zones. Wood frame construction represents the vast majority of residential structures in North America and is gradually gaining acceptance in the Chinese market. In order to either push the current design codes toward the performance assessment level in North America or to fill in the gaps of Chinese timber design codes, seismic evaluation methods based on the structural performance of wood frame construction must be developed.

The development of evaluation methods and design philosophies for structural performance under seismic loading primarily focuses on steel and reinforced concrete structures. In the late 1990s and early 2000s, the application of performance-based design/evaluation methods to wood structures saw substantial progress. Filiatrault and Folz (2002) outlined the limitations of the force-based seismic design procedure for wood frame construction and proposed the application of performance-based seismic design for wood frame construction through a direct-displacement methodology. Rosowsky and Ellingwood (2002), van de Lindt and Walz (2003), and Ellingwood et al. (2004) proposed a fragility-based design method for wood frame construction, where the performance indicator focused on the drift. van de Lindt (2005) proposed a damage-based seismic reliability concept for wood frame construction. The mechanistic damage model expressed damage as a linear combination of the maximum displacement during an earthquake simulation and the hysteretic energy dissipated by each shear wall within a structure. van de Lindt and Dao (2009) proposed performance-based wind engineering design for wood frame construction. Data from nail tests were used in a detailed finite element (FE) model to evaluate the uplift capacity for panels having different nail patterns and truss spacing. Van de Lindt et al. (2013) proposed performance-based seismic design for mid-rise wood frame buildings. The approach relied on a simplified direct displacement design procedure for shear wall selection and a combination of software and basic statics for shear transfer and uplift control. Based on this design method, a 6-story wood frame construction was built and tested in Miki City, Japan, and damage at the maximum credible earthquake level was found to satisfy the performance expectations.

One of the tools used in the seismic evaluation of wood frame construction are numerical models that can predict structural responses. Folz and Filiatrault (2001a) proposed a simple numerical model that was later incorporated into the computer program Seismic Analysis of Wood Framed Structures (SAWS) to predict the dynamic characteristics of wood framed construction. The model was composed of two primary components: rigid horizontal diaphragms and nonlinear lateral load resisting shear wall elements. The degrading strength and stiffness behavior of shear wall elements were represented by an equivalent nonlinear shear spring element. The parameters of the spring elements could be deduced via wood frame shear wall test data or numerical results calculated by the computer program Cyclic Analysis of Shear Walls (CASHEW) (Folz and Filiatrault 2004a, b). The results clearly show that the nonlinear behavior of wood frame construction is mainly governed by the nail connection. Xu and Dolan (2009a, b) modified a general hysteretic model, namely, the Bouc-Wen model, to represent the hysteretic behavior of a nail joint. In that model, 13 hysteretic shape parameters were identified from the results of a series of nail connection tests using genetic algorithms. Then, a detailed shear wall was modeled, therein showing good agreement between the analysis results and test data. Humberta et al. (2014) proposed a constitutive law for nail joints based on a multi-scale concept, therein presenting 9 parameters that govern the behavior under monotonic loading and 4 parameters that govern the shape of hysteresis loops. Over 300 experimental tests were conducted on joints and used to calibrate the constitutive law. A total of 14 experimental tests were performed on different shear wall configurations and were used to validate the proposed FE model. Both monotonic and cyclic test results were in good agreement with the FE model predictions. Foschi (2000) proposed a mechanical hysteretic model for nail joints using basic material properties of the connector and

the embedment characteristics of the surrounding wood medium. This approach considered a nail connector as an elastic-plastic beam acting on wood (modeled as a nonlinear medium that only acted in compression), permitting the formation of gaps between the nail and the wood. The model can be used under various loading protocols, whereas common empirical models mostly only fit well in the given experimental loop. However, the model is very computational intensive because it requires the solution of a nonlinear problem to be generated at each time step.

The numerical models can be used to thoroughly analyze the nail connection, from which the main nonlinearity of the wood frame construction originates. However, the aforementioned seismic evaluation methods primarily focus on the macro structural response, such as drift, uplift and hysteretic energy dissipation, but rarely involve the nail performance status. Applying the advantages of the numerical models, the concept of a seismic evaluation method for wood frame construction based on the nail connection performance status is presented in this paper. An empirical nail connection model adjusted using an energy equivalence principle is proposed to capture the responses under seismic loading. As an application example, a pushover analysis is conducted on an FE model of a wood frame construction with a practical configuration. The main objective of this study is to propose a seismic evaluation method for wood frame construction based on nail connection performance status.

MATERIALS AND METHODS

In this paper, monotonic tests and adjustments referring to an energy equivalence principle are applied to obtain the constitutive relationship of the nail connection. Although the constitutive relationship from the monotonic tests did not set load paths to describe unloading, reloading, and load reversal, it can be effectively used for static nonlinear pushover analysis. The nail connection performance status is classified into four stages based on different deflection levels. Then, two three-dimensional (3D) FE models (parallel and perpendicular to the lumber grain) of wood frame constructions are established based on the nail connection model and are validated with the experimental test results.

Nail connection tests

To obtain the force-deflection relationship of the nail connection, monotonic tests were conducted. Oriented strand board (OSB) with a density of 650 $kg \cdot m^{-3}$ was used as sheathing panels and spruce-pine-fir (SPF) lumber with a density of 470 $kg \cdot m^{-3}$ was used for studs; the moisture content of the OSB panels and the SPF lumber were 20% and 15% respectively during the tests. The specimen types are shown in Tab. 1. The general test setups and the experimental results are shown in Fig. 1.

Tab. 1: Specimen types.

Specimen series	Thickness of OSB panel (mm)	Sectional dimension of nail (mm)	Forced direction to SPF lumber grain	Number of tests
A	9.5	3.3×63	Parallel	15
B			Perpendicular	15

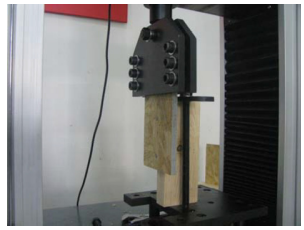

(a) Test setup of Series A

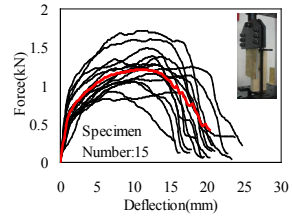

(b) Test results of Series A

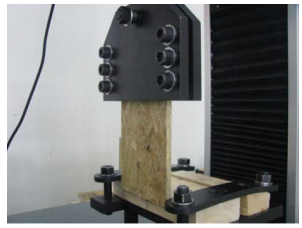

(c) Test setup of Series B

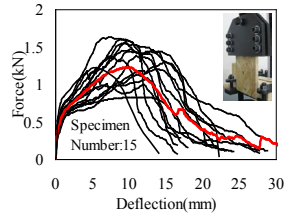

(d) Test results of Series B

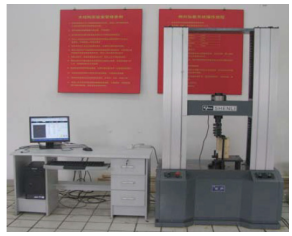

(e) Test loading system

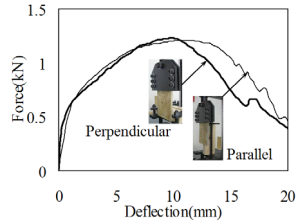

(f) Mean value curves of the experimental results

Fig. 1: Nail connection tests.

Nail connection model establishment

Because the force direction of the nail connection varied throughout the loading process, a pair of springs (one parallel to the lumber grain direction and the other perpendicular to the lumber grain direction) was adopted to model the nail connection. The force and deflection were assumed to follow the rule of vector synthesis (Andreasson 2000).

In the experimental tests, Series A was used to model the spring parallel to the lumber grain, and Series B was used to model the spring perpendicular to the lumber grain. According to the mean value curves of Series A and Series B, the stiffness and the bearing capacity of the nail connection were nearly equal in both directions, and this consistency was also noted in Eurocode 5 - 2004. Hence, in this paper, one force-deflection relationship was applied to springs in both directions.

An empirical spring model was adopted based on the experimental test results. The force-deflection relationship fitted the mean value curve of the test results using a five-parameter function (Fig. 2). This nonlinear model was proposed by Girhammar and Bovirn (2000) and improved upon Foschi's three-parameter model (1974); the function is as follows:

$$F_n = (F_{n0} + K_{n1}\delta_n) \times [1 - e^{-(K_{n0}\delta_n)/F_{n0}}] \times e^{-(\delta_n^{\kappa}/\lambda)} \quad (1)$$

where: F_n - load,
δ_n - deflection,
K_{n0} - initial stiffness,
K_{n1} - stiffness at large deflection,
F_{n0} - intercept of the asymptote with slope K_{n1},
κ, λ - parameters for descending segment.

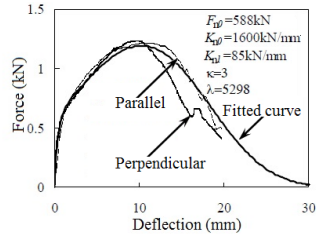

Fig. 2: Fitted curve for the spring model.

When the nail connection model becomes nonlinear, the assumption that the pair of springs operate in accordance with the rules of vector synthesis would overestimate the connection stiffness and bearing capacity. To compensate for this overestimation, Folz and Filiatrault (2000, 2001b) proposed a method of adjustment for the connection model; the force value under a certain displacement should be reduced to a level whereby the energy absorbed using the non-oriented spring pair (Eu, Ev) agreed with the energy absorbed using a single oriented spring (Ed) (Fig. 3). This modification method was subsequently implemented in the SAWS and CASHEW programs.

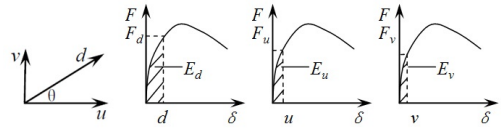

Fig. 3: Diagrammatic sketch of energy absorption.

To address the energy over-prediction, a modification method was applied to adjust the nail connection model. A parameter m was defined to adjust the spring force-deflection relationship (i.e., to multiply the data of the force axis).

$$m = \frac{E_d}{E_u + E_v} \quad (2)$$

The relationship among the adjustment parameter (m), the force angle (θ), and a given displacement (d) is shown in Fig. 4. The figure reveals that the energy over-prediction increases with increasing total displacement. Another notable result is that m appeared to reach a minimum when θ equaled 45° for any given displacement. According to Cassidy (2000), nails in the corners of sheathing panels are the most highly rotated nails and are also the nails that would be oriented most closely to an angle of 45°. There were hundreds of nail connections in the 3D FE model, and it was impossible to adjust every nail connection with different modifiers. Therefore, a mean value of m corresponding to θ ranging from 0° to 45° when d was equal to 10 mm was adopted to modify all the nail connection models; m equaled 0.87.

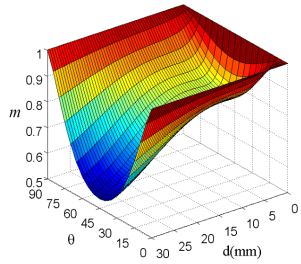

Fig. 4: Relationship among m, θ, and d.

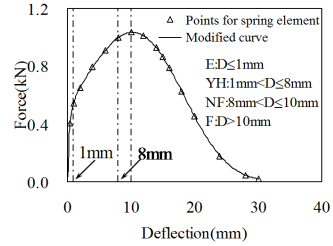

Fig. 5: Adjusted nail connection force-deflection curve.

The adjusted force-deflection curve is shown in Fig. 5. Points on the constitutive relationship curve were used to define the spring elements in the numerical simulation. Throughout the loading process, four stages of nail connection performance status were defined, namely, elastic behavior (E), yielding and hardening (YH), near failure (NF), and failure (F), and the stages were used in the seismic performance evaluation of wood frame constructions in the later section.

FE model establishment and validation

Fig. 6 shows the 3D FE model established using the commercial finite element program ANSYS using the above-described method. Both of the models were symmetric in the X and Y directions and had dimensions of 6.1 m (length) × 6.1 m (width) × 4.88 m (height); the configurations are detailed in Kang et al. (2010). Tab. 2 lists the material properties of the components.

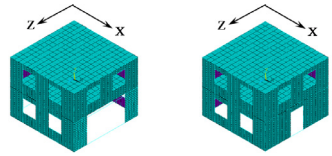

(a) Model I (b) Model II

Fig. 6: 3D FE model.

Tab. 2: Modulus of elasticity for components (MPa.)

9.5-mm-thick OSB		Joist	Header at door opening	Stud
long side direction	Short side direction			
5.2×10^3	2.6×10^3	2.8×10^4	1.2×10^5	9.5×10^3

To validate the 3D FE models, lateral loading was applied in the X direction at an elevation corresponding to the first story through numerical simulation and experimental tests (Fig. 7) (Kang et al. 2010). The force-deformation curves of the modeling were adopted for comparison with the backbone of hysteretic loops in the experimental tests (Fig. 8).

Fig. 7: Experimental test setup.

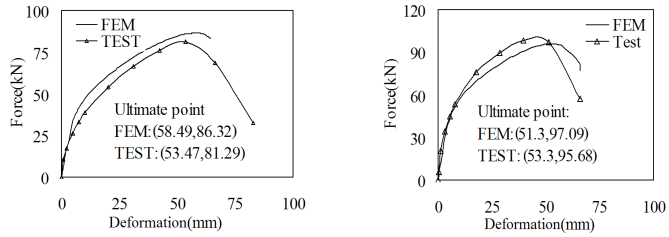

(a) Model I (b) Model II

Fig. 8: FE model validation.

RESULTS AND DISCUSSION

Fig. 8 shows that the FE model predicted the maximum force and corresponding deformation reasonably well and that the accuracy was acceptable. The FE model was able to capture the entire structure response under monotonic load. In this section, analysis and evaluation are performed on Model II in the X direction.

Firstly a pushover analysis is conducted on the 3D FE model; then, the force-deformation curve is transferred to an idealized bilinear curve and converted into an equivalent capacity curve in spectral acceleration (Sa) and spectral displacement (Sd) format. Performance parameters under different seismic hazard levels are obtained using the capacity-demand-diagram method.

Dynamic parameters

First, a modal analysis is conducted on the 3D FE model. Parameters for conversion from the pushover curve to an equivalent capacity curve, such as the first frequency (f_1), first mode shape ratios (ϕ_1), effective modal mass (M_1^*) and participation factor (Γ_1), are listed in Tab. 3. The first mode shape of the X direction is shown in Fig. 9.

Tab. 3: Dynamic parameters of the FE model in X direction.

$\phi_{1,1}$	$\phi_{1,2}$	M_1^* (t)	Γ_1	f_1(H)
0.17	0.29	19.82	4.45	2.72

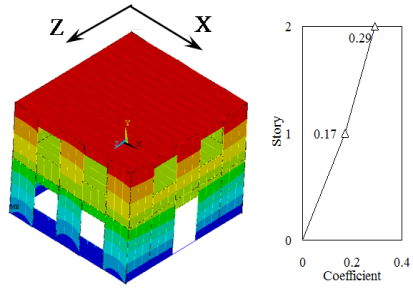

Fig. 9: First mode shape of Model II in X direction.

Performance parameters under different seismic hazard levels

Pushover analysis was conducted on the 3D FE model II in the weak direction, namely, the X direction. The pushover curve, namely, the relationship curve between the base shear (V_b) and roof deformation (Δ_{roof}), is shown in Fig. 10. The pushover curve was transferred to an idealized bilinear curve according to Federal Emergency Management Agency (FEMA) 273 (FEMA 1997) and ASTM E2126, 2012. Then, all points (Δ_{roof}, V_b) on the bilinear curve were converted to the corresponding points (S_d, S_a) on the capacity spectrum (Fig. 11) using the equations below:

$$S_a = V_b / M_1^* \tag{3}$$

$$S_d = \Delta_{\text{roof}} / (\Gamma_1 \phi_{1,2}) \tag{4}$$

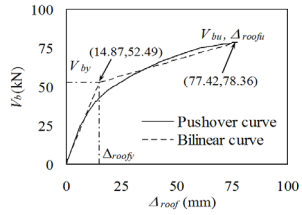

Fig. 10: Pushover curve and the idealized bilinear curve.

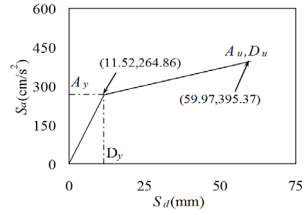

Fig. 11: Capacity spectrum curve.

For the demand spectrum curve, referring to Chinese Standard GB 50005-2003 (China Ministry of Construction 2003) and GB 50011-2010 (China Ministry of Construction 2010), the seismic hazard level was chosen as intensity 7, and the seismic spectrum could be determined as follows:

$$S_a = \alpha \mathrm{g} = \begin{cases} [10(\eta_2 - 0.45)T + 0.45]\alpha_{\max}\mathrm{g} & 0 < T < 0.1 \\ \eta_2 \alpha_{\max}\mathrm{g} & 0.1 \le T < T_g \\ (\frac{T_g}{T})^{\gamma} \eta_2 \alpha_{\max}\mathrm{g} & T_g \le T < 5T_g \\ [\eta_2 0.2^{\gamma} - \eta_1 (T - 5T_g)]\alpha_{\max}\mathrm{g} & 5T_g \le T \le 6.0 \end{cases} \tag{5}$$

where: g - acceleration of gravity,

α - seismic effect coefficient,

$\alpha_{\max}$ - maximum seismic effect coefficient under seismic hazard level of intensity 7 [occasional earthquake (OE, return period: 72 years): 0.12; rare earthquake (RE, return period:

474 years): 0.34; very rare earthquake (VRE, return period: 2475 years): 0.72],

ζ - damping ratio (wood frame construction: 0.05),

γ - attenuation index (0.9); η_1 = slope adjustment factor (0.02),

η_2 = damping adjustment factor (1.0),

T = structural period ($T = 1/f_1$),

T_g = site characteristic period (three different site classes: 0.20 s, 0.55 s, and 0.90 s).

The improved capacity-demand-diagram method developed by Chopra and Goel (1999) is adopted in this paper. The seismic spectrum was converted to an inelastic demand spectrum in Sa-Sd format, and the capacity spectrum was plotted in the same coordinates to obtain the performance point. The seismic performance parameters of the wood frame construction are listed in Tables 4~6.

Tab. 4. Seismic performance parameters under OE.

T_g (s)	S_a (g)	S_d (mm)	Inter-story deformation (mm)		Inter-story shear force (kN)	
			Second story	First story	Second story	First story
0.20	0.06	2.7	1.7 (0.07%)	1.8 (0.07%)	9.21	13.82
0.55	0.12	5.2	2.9 (0.12%)	3.6 (0.15%)	16.90	25.36
0.90	0.12	5.2	2.9 (0.12%)	3.6 (0.15%)	16.90	25.36

Tab. 5: Seismic performance parameters under RE.

T_g (s)	S_a (g)	S_d (mm)	Inter-story deformation (mm)		Inter-story shear force (kN)	
			Second story	First story	Second story	First story
0.20	0.18	7.5	4.3 (0.17%)	5.4 (0.22%)	22.21	33.31
0.55	0.28	14.1	7.0 (0.28%)	11.2 (0.46%)	31.16	46.74
0.90	0.28	15.2	7.4 (0.30%)	12.2 (0.50%)	32.18	48.28

Tab. 6: Seismic performance parameters under VRE.

T_g (s)	S_a (g)	S_d (mm)	Inter-story deformation (mm)		Inter-story shear force (kN)	
			Second story	First story	Second story	First story
0.20	0.28	15.5	7.5 (0.30%)	12.5 (0.51%)	32.47	48.70
0.55	0.32	29.5	12.5 (0.51%)	25.6 (1.04%)	42.07	63.11
0.90	0.35	39.9	16.4 (0.67%)	35.1 (1.43%)	47.06	70.59

Note: The number in parentheses indicates the inter-story deformation ratio.

Seismic evaluation based on nail connection performance status

FEMA 273 suggests values and expected performance limit states based on seismic hazard levels, as shown in Tab. 7. In this section, the expected performance levels are adopted as the performance indicators to facilitate the seismic evaluation. The distribution of nail connections under different performance statuses is captured corresponding to the deformation of the entire construction, and the relationship curve is shown in Fig. 12.

Tab. 7: Performance under different seismic hazard levels for wood frame construction.

Seismic hazard level	Seismic design performance level		
	Immediate occupancy	Life safety	Collapse prevention
Occasional Earthquake Return Period: 72 years	Drift limits: 1% transient 0.25% permanent	-	-
Rare Earthquake Return Period: 474 years	-	Drift limits: 2% transient 1% permanent	-
Very Rare Earthquake Return Period: 2475 years	-	-	Drift limits: 3% transient or permanent

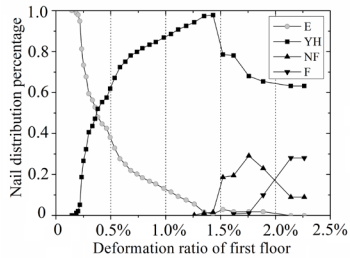

Fig. 12: Nail distribution with structural deformation.

When the studied structure was subjected to an occasional earthquake, the maximum inter-story deformation ratio was 0.15%, which occurred in the first story, thereby meeting the 1% transient and 0.25% permanent tolerance of the FEMA 273. When the deformation ratio of the first story was less than 0.15%, all the nail connections in the wall were in the E stage, namely, the maximum nail connection deflection was smaller than 1 mm. The relatively small inter-story deformation ratio would cause minimal cracking of the gypsum board according to McMullin and Merrick (2007), and thus, the structure could be classified as immediate occupancy.

When the studied structure was subjected to a rare earthquake, the inter-story deformation ratio of the first story was 0.50%, which is under the 2% transient and 1% permanent tolerance of FEMA 273; the distribution of the different nail connection statuses is shown in Fig. 13. The nail connections in the YH stage were mainly located around the perimeter of the OSB sheathings; the relatively large deflection of the nail connections appeared at the corner of the OSB sheathing and around the compressive regions of the studs, sill plates and headers of window openings. A total of 62% of the nail connections in the first story and 23% of the nail connections in the second story were present in the YH stage, indicating that loosening of the nail connections occurred. As the inter-story deformation ratio increased to 0.50%, cracking of the gypsum board was obvious. On the other hand, none of the nail connections were found in the NF stage, and the maximum nail deflection was less than 3 mm. As a result, the connection loosening would be limited to a moderate degree, and the life safety of the structure could be ensured.

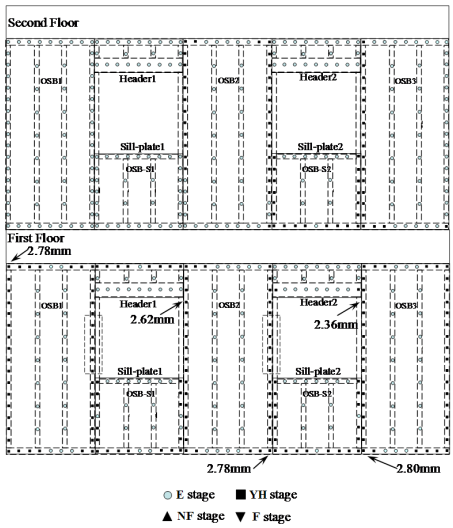

Fig. 13: Distribution of nail connections under different performance statuses (First story deformation ratio: 0.5%).

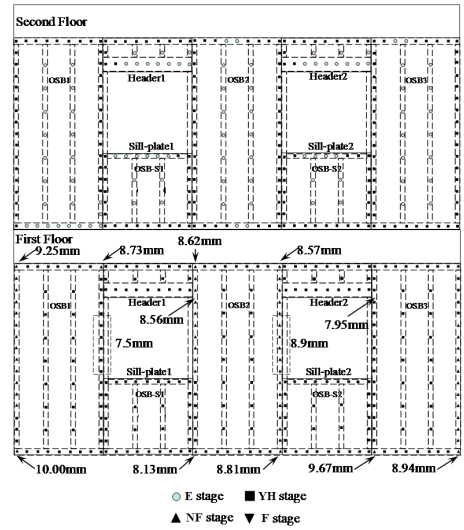

Fig. 14: Distribution of nail connections under different performance statuses (First story deformation ratio: 1.43%).

Under very rare earthquake conditions, the deformation ratio of the first story reached 1.43%, and the distribution of the different stage nail connections is shown in Fig. 14. In the second story, the nail connections around the OSB sheathing were found in the YH stage (63% of all nail connections). In the first story, only 10% of the nail connections remained in the E stage; thus, the nonlinearity of the construction was substantial. The maximum nail deflection of the first story was approximately 9.7 mm, and non-structural components would be heavily damaged. However, only 18% of the nail connections of the first story were found in the NF stage, without any reaching the F stage. Thus, the OSB sheathing would not become completely detached from the frame and would continue to partially function with the framing. Because the maximum inter-story deformation ratio was under the limit value of 3% of FEMA 273 and because the lateral resistance of the shear wall would be partially maintained, the studied structure could achieve the collapse prevention standard under this seismic hazard level.

From the above discussion, the proposed method was able to capture the entire structural response and facilitate detailed analyses on the nail connection performance status. Besides, other performance standards in addition to FEMA 273 (e.g., specific requirements of the owners) are also applicable when using this evaluation method.

CONCLUSIONS

In this paper, the concept for a seismic evaluation method for wood frame construction based on nail connection performance status was presented. An empirical nail model adjusted using an energy equivalence principle was proposed to capture the nail connection responses under seismic loading. An application example of wood frame construction with a practical configuration was presented and evaluated through pushover analysis. Taking FEMA 273's seismic design

performance levels, which were associated with different hazard levels, as the performance indicators, a seismic evaluation was conducted on a wood frame construction. The proposed method was able to capture the entire structural response based on the detailed analyses of the nail connection performance status.

ACKNOWLEDGMENTS

The authors are grateful for the financial support from the Key University Research Project of the Education Department of Henan Province (Grant no. 18A560003) and the China Postdoctoral Fund (Grant no. 2018M632804).

REFERENCES

1. Andreasson, S., 2000: Three-dimensional interaction in stabilization of multi-storey timber frame building systems. Ph.D. thesis, Lund University, Lund, Sweden.
2. ASTM E2126-11-2012: Standard test methods for cyclic (reversed) load test for shear resistance of vertical elements of the lateral force resisting systems for buildings.
3. Cassidy, E.D., 2000: Development and structural testing of FRP reinforced OSB panels for disaster resistant construction. Master's thesis, University of Maine, Orono, ME.
4. GB 50005-2003. 2003: Code for design of timber structures.
5. GB 50011-2010. 2010: Code for seismic design of buildings.
6. Chopra, A.K., Goel, R.K., 1999: Capacity-demand-diagram methods based on inelastic design spectrum, Earthquake Spectra 15 (4): 637-655.
7. CEN 2004: Eurocode 5: Design of timber structures. Part 1-1: general-common rules and rules for buildings.
8. Ellingwood, B.R., Rosowsky, D.V., Li, Y., Kim, J.H., 2004: Fragility assessment of light-frame wood construction subjected to wind and earthquake hazards, Journal of Structural Engineering 130 (12): 1921-1930.
9. Federal Emergency Management Agency. 1997: NEHERP guidelines for the seismic rehabilitation of buildings. FEMA 273. Washington, DC: FEMA.
10. Filiatrault, A., Folz, B., 2002: Performance-based seismic design of wood framed buildings, Journal of Structural Engineering 128 (1), 39-47.
11. Folz, B., Filiatrault, A.,2000: CASHEW-Version 1.0: a computer program for cyclic analysis of wood shear walls. Structural Systems Research Project, Report No. SSRP-2000/10, Department of Structural Engineering, University of California, San Diego, La Jolla, CA.
12. Folz, B., Filiatrault, A, 2001a: Cyclic analysis of wood shear walls, Journal of Structural Engineering 127 (4): 433-441.
13. Folz, B., Filiatrault, A., 2001b: SAWS-Version 1.0: a computer program for seismic analysis of wood frame buildings, Structural Systems Research Project, No. SSRP-2001/9, Department of Structural Engineering, University of California, San Diego, La Jolla, CA.
14. Folz, B., Filiatrault, A., 2004a: Seismic analysis of woodframe structures. I: model formulation, Journal of Structural Engineering 130 (9): 1353-1360.
15. Folz, B., Filiatrault, A., 2004b: Seismic analysis of woodframe structures. II: model implementation and verification, Journal of Structural Engineering 130 (9): 1361-1370.

16. Foschi, R.O. 1974: Load-slip characteristics of nails, Wood Science 7 (1): 69-74.
17. Foschi, R.O., 2000: Modeling the hysteretic response of mechanical connections for wood structures. Proc., 2000 World Conf. on Timber Engineering, Whistler, B.C. Canada.
18. Girhammar, U, A., Bovirn, N, I., 2000: Characteristics of sheathing-to-timber joints in wood shear walls. Proc., 2000 World Conf. on Timber Engineering, Whistler, B.C. Canada.
19. Humbert, J., Boudaud, C., Baroth, J., Hameury, S., Daudeville, L., 2014: Joints and wood shear walls modelling I: Constitutive law, experimental tests and FE model under quasi-static loading, Engineering Structures 65: 52-61.
20. Kang, J., Xiong, H., Lu, X., 2010: Cyclic tests of full-scale wood framed constructions, China Civil Engineering Journal 43 (11): 71-78.
21. McMullin, K., Merrick, D., 2007: Seismic damage thresholds for gypsum wallboard partition walls, Journal of Architectural Engineering 13 (1): 22-29.
22. Rosowsky, D.V., Ellingwood, B.R., 2002: Performance-based engineering of wood frame housing: a fragility analysis methodology, Journal of Structural Engineering 128 (1): 32-38.
23. Van de Lindt, J.W., Walz, M.A., 2003: Development and application of wood shear wall reliability model, Journal of Structural Engineering 129 (3): 405-413.
24. Van de Lindt, J.W., 2005: Damage-based seismic reliability concept for woodframe structures, Journal of Structural Engineering 131 (4): 668-675.
25. Van de Lindt, J.W., Dao, T., 2009: Performance-based wind engineering for wood-frame buildings, Journal of Structural Engineering 135 (2): 169-177.
26. Van de Lindt, J., Rosowsky, D., Pang, W., Pei, S., 2013: Performance-based seismic design of midrise woodframe buildings, Journal of Structural Engineering 139 (Special Issue), 1294-1302.
27. Xu, J., Dolan, J., 2009a: Development of nailed wood joint element in ABAQUS, Journal of Structural Engineering 135 (8): 968-976.
28. Xu, J., Dolan, J., 2009b: Development of a wood-frame shear wall model in ABAQUS, Journal of Structural Engineering 135 (8): 977-984.

Yingyang Liu*
Zhengzhou University
School of Civil Engineering
No.100 Science Avenue
Zhengzhou 450001
China
Phone: +86-371-67781680
*Corresponding author: liuyingyang5687@qq.com

Haibei Xiong
Tongji University
Shanghai 200092
China

Jiahua Kang
Architectural Design & Research Institute of Tongji University (Group)
Co., Ltd.
Shanghai 200092
China